Tumor Necrosis Factor-α Modifies Adhesion Properties of Rat Islet B Cells

Vincenzo Cirulli, Philippe A. Halban, and Dominique G. Rouiller
Laboratoires de Recherche Louis Jeantet, Centre Médical Universitaire, CH-1211 Geneva 4, Switzerland

Abstract

The characteristic three-dimensional cell type organization of islets of Langerhans is perturbed in animal models of diabetes, suggesting that it may be important for islet function. Rat islet cells in culture are able to form aggregates with an architecture similar to native islets (pseudoislets), thus providing a good model to study the molecular basis of islet architecture and its role in islet function. Sorted islet B cells and non–B cells were permanently labeled with two different fluorescent dyes (DiO and DiI), mixed, and allowed to form aggregates during a 5-d culture in the presence or absence of TNF-α (100 U/ml), a cytokine suggested to be implicated in the early physiological events leading to insulin-dependent diabetes mellitus. Confocal microscopy of aggregates revealed that TNF-α reversibly perturbs the typical segregation between B and non–B cells. Insulin secretion, was altered in the disorganized aggregates, and returned towards normal when pseudoislets had regained their typical architecture. The homotypic adhesion properties of sorted B and non–B cells cultured for 20 h in the presence or absence of TNF-α were studied in a short term aggregation assay. TNF-α induced a significant rise in Ca^{2+}-independent adhesion of B cells (from 24±1.1% to 44.3±1.2%; $n = 4$, $P < 0.001$). These findings raise the possibility that the increased expression of Ca^{2+}-independent adhesion molecules on B cells leads to altered islet architecture, which might be a factor in the perturbation of islet function induced by TNF-α. (*J. Clin. Invest.* 1993. 91:1868–1876.) Key words: tumor necrosis factor-α • cell adhesion • rat islet B cells • islets of Langerhans • insulin-dependent diabetes mellitus

Introduction

Cells are nonrandomly distributed within islets of Langerhans. In the rat, islets are formed as a core of insulin-secreting B cells surrounded by the three other cell types, A, D, and PP, secreting glucagon, somatostatin, and pancreatic polypeptide, respectively (1). This typical topographical arrangement of cells within the islet is perturbed in all forms of diabetes that have been studied (2–7), suggesting that it may be important for islet function.

When rat islet cells are dissociated with trypsin and allowed to reaggregate in culture, they form islet-like structures, with B cells in the center surrounded by a rim of non–B cells (8–10). Such "pseudoislets" have been proposed as a model to study the influence of islet cell interrelationships upon islet function (9–12). The ability of islet cells to form islet-like organoids suggests a cell type–specific expression of cell adhesion molecules (CAMs)[1] responsible for selective recognition/adhesion and segregation between B and non–B cells. Indeed, sorted islet non–B cells express significantly higher levels of Ca^{2+}-independent CAMs compared to B cells, while E cadherin (uvomorulin), a Ca^{2+}-dependent CAM, is identically expressed on both cell types (13, 14). Furthermore, incubation of cells with antibodies directed against Ca^{2+}-independent CAMs profoundly perturbs the cellular organization of pseudoislets (14).

Cytokines secreted by leukocytes infiltrating the islets have been implicated in the early events leading to diabetes (15–19). Furthermore, the cytokine TNF-α has been shown to induce the expression of a CAM, the intercellular CAM-1 (ICAM-1), on pancreatic endocrine B cells (20, 21). Thus, in addition to allowing the attachment of cytotoxic lymphocytes, this cytokine might initiate islet dysfunction by the induction of unusual CAMs, with the resulting loss of islet cell type segregation, or by modifying the expression of constitutive CAMs responsible for normal cell type adhesion and segregation.

In the present work, we show that TNF-α reversibly perturbs the cellular organization within pseudoislets, together with a reversible alteration of basal and glucose-induced insulin secretion. To gain more insight into the molecular basis of the effect of TNF-α on islet architecture, we also studied the effect of the cytokine on the homotypic adhesion properties of sorted islet B and non–B cells. The results show that TNF-α increases the Ca^{2+}-independent homotypic adhesion of B cells. It is suggested that this increase is responsible for the altered pseudoislet cellular organization.

Methods

Islet isolation. Pancreatic islets were isolated from Sprague-Dawley rats (weighing 200–250 g) by a modification of the method of Sutton et al. (22), as previously described (13). The yield was about 800 islets per rat.

Preparation of islet cells. Freshly isolated islets were washed twice with Mg^{2+}-, Ca^{2+}-free PBS containing 0.5 mM EDTA and resuspended into 1.5 ml of Puck's buffer containing 0.16 mg/ml of trypsin (activity against casein, 1:250) and 0.1 mM EDTA. Digestion was carried out for 6–7 min at 37°C until only few doublet cells remained. The reaction was ended by adding 10 ml ice-cold Krebs-Ringer bicarbonate (KRB) buffer, pH 7.4, containing 0.5% BSA, 2.5 mM glucose, and 10 mM Hepes. After centrifugation for 8 min at 4°C and 600 *g*,

Address correspondence to Vincenzo Cirulli, M.D., Laboratoires de Recherche Louis Jeantet, Centre Médical Universitaire, 1 rue Michel Servet, CH-1211 Geneva 4, Switzerland.

Received for publication 19 December 1991 and in revised form 20 November 1992.

J. Clin. Invest.
© The American Society for Clinical Investigation, Inc.
0021-9738/93/05/1868/09 $2.00
Volume 91, May 1993, 1868–1876

1. *Abbreviations used in this paper:* CAMs, cell adhesion molecules; DiI, 1,1′dioctadecyl-3,3,3′,3′-tetramethyl-indo-carbocyanine perchlorate; DiO, 3,3′-dioctadecyl-oxa-carbocyanine perchlorate; ICAM-1, intercellular adhesion molecule-1; IDDM, insulin-dependent diabetes mellitus; KRB, Krebs-Ringer bicarbonate; LFA-1, lymphocyte-function associated antigen-1; NCAM, neural cell adhesion molecule; NIDDM, non-insulin-dependent diabetes mellitus; TC treatment, trypsin treatment in the presence of Calcium; TE treatment, trypsin treatment in the presence of EDTA.

cells were taken up in the same buffer to a final concentration of 3 $\times 10^6$ cells/ml. The yield was 1–1.5 $\times 10^6$ cells per pancreas.

Autofluorescence-activated cell sorting of islet B- and non–B cells. Dispersed islet cells were analyzed in an Epics-V flow cytometer connected to a Multidisplay Acquisition Data System microcomputer (Coulter Electronics, Hialeah, FL). Cellular autofluorescence, excited by an argon laser beam tuned to 488 nm at 500–600 mW output power, was plotted against forward light scatter, which relates to cellular size (23). As reported (24), at 2.5 mM glucose, two islet cell populations became apparent when particle flavin adenine dinucleotide autofluorescence (510–550 nm) was plotted against light scatter. Sorting "windows" were then externally applied around both populations in order to deflect viable cells into one or the other collecting tube containing sterile KRB-BSA.

The distribution of insulin and glucagon containing cells was assessed by classical double antibody cytochemistry (25). As recently described (13), following this procedure, one sorted population contained 93±1.6% non–B cells, and the other population contained 95±0.7% B cells. About 1 million non–B cells and 2.8 million B cells were obtained from six rats.

Islet cell culture. For the short-term aggregation assay, sorted β cells were resuspended in DME (Gibco Laboratories, Grand Island, NY), containing 5% FCS, 5 mM glucose, with or without 100 U/ml of mouse recombinant TNF-α (kindly provided by BASF & Knoll Aktiengesellschaft, Ludwigshafen, Germany). Cells were seeded in 100-mm nonadherent petri dishes (model no. 1007; Falcon, Oxnard, CA) at a concentration of 2×10^4 cells/ml to prevent their premature reaggregation, and kept for 20 h in a humidified atmosphere of 95% air and 5% CO_2 at 37°C to allow them to fully regenerate any lost or damaged cell surface proteins.

Colorimetric pseudoislet assay. The method recently proposed by Friedlander et al. (26) to study the sorting out of mouse cells, was used to investigate islet cell type segregation during pseudoislet formation in vitro (14): sorted islet cells were differentially labeled with the vital fluorescent dyes 3,3′-dioctadecyl-oxa-carbocyanine perchlorate (DiO) and 1,1′-dioctadecyl-3,3,3′,3′-tetramethyl-indo-carbocyanine perchlorate (DiI) (Molecular Probes, Inc., Eugene, OR). These compounds have a high affinity for lipids, are nontoxic to the cells, and provide an intense cell fluorescence which fades much more slowly than either fluorescein or rhodamine. DiI is maximally excited by green light and fluoresces red-orange when viewed through rhodamine filters, while DiO is excited in the blue and fluoresces green when observed through fluorescein filters. Membranes labeled with these tracers retain the fluorescence for several days, even weeks (27). After cell sorting, islet B and non–B cells were separately incubated in DME containing 5 mM glucose, 5% FCS, and either 3 μg/ml of DiI (B cells) or 10 μg/ml of DiO (non–B cells) for a period of 18–20 h, at a dilution of 3×10^4 cells/ml to avoid premature reaggregation. At the end of this labeling/culture period, cells were washed three times with fresh medium to eliminate unbound dye. The two cell populations were mixed together at a ratio of 60% non–B cells and 40% B cells, to account for the smaller size of non–B cells, and resuspended at a concentration of 2×10^6 cells/ml in DME containing 5 mM glucose, 10% FCS, 10 mM Hepes, with or without 100 U/ml of mouse recombinant TNF-α. They were then placed in 35 × 10-mm nonadherent petri dishes as microdroplets of 40 μl each, and incubated overnight in a humidified atmosphere of 95% air and 5% CO_2 at 37°C. The next day, clusters were diluted by adding 3 ml of fresh medium with or without 100 U/ml TNF-α. Samples to be studied for the effect of the cytokine were supplemented with 100 U/petri ($\sim$ 30 U/ml) of fresh TNF-α at the end of days 3 and 4 to account for TNF-α degradation (18, 28). Cell type segregation and organization within the pseudoislets were monitored at day 5 by laser fluorescence microscopy using a confocal imaging system (MRC-600; Bio-Rad Laboratories, Microscience Division, Watford, UK). Samples were examined through a dual channel system using a green 514-nm argon ion laser line for excitation of both DiO and DiI fluorochromes, applying the filter combination A1/A2 (Bio-Rad Laboratories). The same day, equivalent samples of control and TNF-α–exposed pseudoislets were washed, replated in fresh medium without the cytokine, and cultured for an additional 3-d period to study the reversibility of the TNF-α effect. On day 8, samples were studied under confocal microscopy for cell type organization.

The partial overlap existing between the emission spectra of the two carbocyanines allowed us to simultaneously identify on the same scanned plane both DiO and DiI fluorescences as different grey levels. Gain and contrast levels were set according to procedures standardized to ensure that the collected image demonstrates a full range of grey level values from black (0-pixel intensity level) to peak white (255-pixel intensity level). Clusters of only non–B cells labeled with the green fluorescent DiO, and clusters of only B cells labeled with the red fluorescent DiI were used as controls to identify the grey band width corresponding to the green (DiO) or red (DiI) fluorescence, respectively. Pseudoislets were then scanned using the Kalman filter, which averages all frames since initiation of image acquisition. Confocal sections corresponding to the equatorial regions of each aggregate were chosen to consistently identify the organization of cells within the core of the pseudoislets. To remove residual noise on the acquired confocal images, the smoothing function of the confocal scanning optical microscopy software was then applied, choosing the s5a patch size, where the letter s symbolizes the smoothing command, the number 5 determines the highest spatial frequencies to be smoothed (second grade of 3, 5, 7, and 9 patch sizes available), and the associated letter a indicates the severity of the operation (a is least). A pseudocolor display of the acquired images was then produced attributing green and red to the DiO and the DiI grey bands respectively using the "band" command of the CSOM's software (Bio-Rad Laboratories).

Glucose-stimulated insulin secretion from pseudoislets. After 5 d in culture, using exactly the same protocol as described above for pseudoislets destined for colorimetric assay, controls, and pseudoislets exposed to TNF-α were hand-picked, washed, and preincubated at 37°C for 1 h in KRB buffer containing a low concentration of glucose (2.8 mM). The pseudoislets were then resuspended and incubated first for 90 min at 37°C in KRB containing 2.8 mM glucose (basal secretion) and then for a further 90 min at 37°C in KRB containing 16.7 mM glucose (stimulated secretion). Insulin in the media, collected at the end of each incubation, and in cells extracted in acid/ethanol was measured by RIA using rat insulin as the standard. The same day, equivalent samples of control and TNF-α–exposed pseudoislets were washed, replated in fresh medium without the cytokine, and cultured for an additional 3-d period to study the reversibility of any TNF-α effect on insulin secretion.

Short-term aggregation assay. At the end of a 20-h culture period, untreated sorted B cells, non–B cells, and cells exposed to TNF-α were applied on top of a discontinuous Percoll gradient (3.5 ml each of isotonic 30 and 60% Percoll) (Pharmacia, Uppsala, Sweden) to eliminate dead cells and cell debris. The viable cells of each sample (harvested from the 30/60% Percoll interface after centrifugation for 10 min at 900 *g*; 24°C) were then divided in two pools that were washed with KRB containing 10 mM glucose, 0.5% BSA, 50 μg/ml DNase (type IV, cat. no. D-5025; Sigma Immunochemicals, St. Louis, MO) and either 1 mM $CaCl_2$ or 0.5 mM EGTA. The cells were then resuspended in 10-ml polycarbonate conical tubes (Nunc, Roskilden, Denmark), in 150 μl of the same buffers at a concentration of 7×10^5 cells/ml. The tubes were then placed at a fixed angle of 30° in a shaking waterbath (100 cycles/min) and incubated at 37°C for 45 min, a time during which a plateau of aggregation is reached (data not shown). At the end of this incubation period, B cell aggregation was assessed in the different samples, both qualitatively using conventional light microscopy and quantitatively by comparing the number of events before and after the aggregation period as measured in a particle counter (ZM Coulter counter; Coulter Electronics, Luton, UK) (13, 14). The extent of aggregation was expressed in percent using the following formula:

$$Aggregation = \frac{(b - a)}{b} \times 100,$$

where b is the number of events before aggregation and a is the number of events counted after the 45-min aggregation period.

In antibody-induced perturbation studies, control and TNF-α–exposed cells were preincubated for 45 min at 4°C with either anti-neural CAM (NCAM) polyclonal antibody (500 μg/ml) (kindly provided by Dr U. Rutishauser, Case Western Reserve University, Cleveland, OH), or anti-rat ICAM-1, anti-rat LFA-1/α, or anti-rat LFA-1/β monoclonal antibodies (10 μg/ml) (kindly provided by Dr. T. Tamatani and Dr. M. Miyasaka, The Tokyo Metropolitan Institute of Medical Science, Tokyo, Japan) (29). As an internal control for nonspecific binding, a sample of cells was preincubated with a nonimmune serum. All samples were then incubated at 37°C for 45 min for aggregation in the absence of calcium (0.5 mM EGTA).

Immuno–flow cytometric analysis. 2.5×10^5 control and TNF-α–treated cells were incubated on ice for 45 min in a volume of 150 μl of KRB buffer containing first 500 μg/ml of anti-NCAM polyclonal antibody (kindly provided by U. Rutishauser), or 10 μg/ml of purified monoclonal antibodies against rat ICAM-1, LFA-1/α, or LFA-1/β (kindly provided by Dr. T. Tamatani and Dr. M. Miyasaka), and second FITC-conjugated appropriate IgG (Tago, Inc., Burlingame, CA) at 1:100 dilution. After washing, cells were analyzed in a flow cytometer (FACScan®; Becton Dickinson, San Jose, CA).

Selective removal of Ca^{2+}-independent CAMs from B cell surface: TC treatment. Takeichi et al. first demonstrated that trypsin treatment can selectively remove either Ca^{2+}-independent or Ca^{2+}-dependent CAMs (also known as cadherins) from the surface of Chinese hamster V79 lung cells, depending on the presence or absence of Ca^{2+}, and on the concentration of trypsin (30). In the presence of Ca^{2+}, cadherins assume a three-dimensional configuration that renders their cleavage sites inaccessible to trypsin, while Ca^{2+}-independent CAMs are digested (TC treatment). We recently demonstrated the usefulness of this procedure for the selective removal of Ca^{2+}-independent CAMs from the surface of islet cells (14): cells were washed with Puck's buffer containing 1 mM $CaCl_2$, and incubated in the same buffer, supplemented with 10 μg/ml trypsin (type I; Sigma Immunochemicals), at 37°C for 15 min. The reaction was ended by adding cold KRB containing 0.3% BSA. The cells were then assessed for their adhesion properties in the short term aggregation assay.

Selective removal of Ca^{2+}-dependent CAMs from B cell surface: TE treatment. As reported (14), the incubation of islet cells with a low concentration of trypsin in the absence of calcium leads to the selective removal of Ca^{2+}-dependent CAMs. Cells were washed in ice-cold KRB without calcium (0.2 mM EDTA) and without BSA, and then incubated in the same buffer containing 1 μg/ml trypsin (type I; Sigma

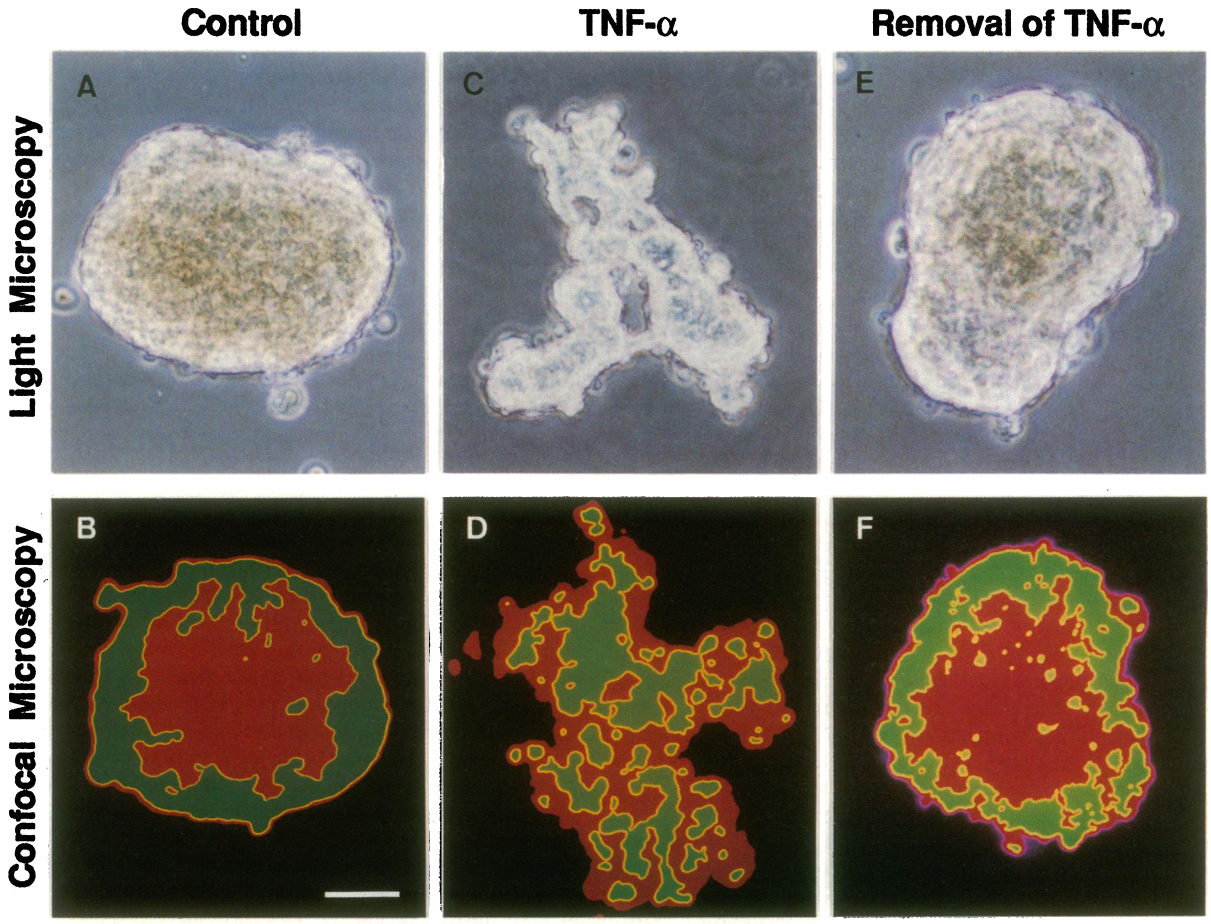

Figure 1. Effect of TNF-α on islet cell type organization. Sorted islet B cells and non–B cells were labeled with the fluorescent carbocyanines, DiI and DiO, respectively. The two differentially labeled populations were then mixed together and allowed to form aggregates in culture over an 8-d period. On day 5, control cells (*A* and *B*) had formed compact pseudoislets with smooth borders, as demonstrated by conventional phase contrast microscopy (*A*). Under confocal fluorescence microscopy, the characteristic sorting out of cells can be appreciated (*B*), with B cells in the center (*red fluorescence*), surrounded by non–B cells (*green fluorescence*); the very thin lines at the periphery are diffusion artefacts of light fluorescence unrelated to cells. In cells cultured for 5 d in the presence of TNF-α (*C* and *D*), the limits of aggregates were ill defined (*C*) and segregation between B and non–B cells did not occur (*D*). On day 5, TNF-α–treated aggregates were transferred to fresh medium without TNF-α. 3 d later (*E* and *F*), aggregates displayed a normal configuration (*E*), with the characteristic segregation between B and non–B cells (*F*), showing that the TNF-α effect is reversible. The figure is representative of a total of six separate experiments. Bar, 50 μm.

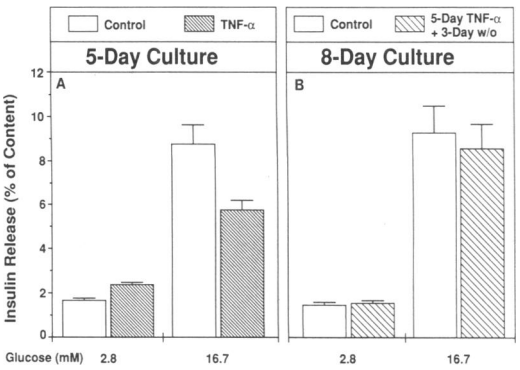

Figure 2. Glucose-stimulated insulin secretion from pseudoislets. After 5 d in culture, control and TNF-α–exposed pseudoislets were incubated with 2.8 and 16.7 mM glucose during two successive 90-min incubation periods to measure basal and stimulated insulin secretion, respectively. The cellular insulin content of pseudoislets in each sample was as follows: 5-d control, 718±221 ng; 5-d TNF-α, 747±200 ng; 8-d control, 642±181 ng; 5-d TNF-α plus 3-d without, 616±178 ng. Insulin release is expressed as a percentage of these cellular insulin contents. Basal insulin release was significantly ($P < 0.002$) elevated from pseudoislets formed in the presence of TNF-α as compared to control (*A*, 2.8 mM glucose). When the glucose concentration in the stimulation medium was raised to 16.7 mM, insulin secretion was significantly ($P < 0.02$) lower from pseudoislets exposed to TNF-α (*A*, 16.7 mM glucose). Pseudoislets incubated for 5 d with TNF-α, followed by 3 d without, showed a normalization of both basal and stimulated insulin secretion (*B*). Bars show the mean±SEM of four independent experiments with each experiment performed in triplicate.

Immunochemicals) for 15 min at 37°C. The reaction was ended by adding cold KRB containing 1 mM $CaCl_2$ and 0.3% BSA. The cells were then assessed for their adhesion properties in the short-term aggregation assay.

Presentation of data and statistics. Data are presented as mean±SEM. The significance for differences between groups was evaluated by Student's two tailed *t* test for paired groups.

Results

Effect of TNF-α on pseudoislet organization. A suspension of islet cells was obtained by mild trypsin digestion of freshly isolated rat islets of Langerhans. B and non–B cells were sorted by flow cytometry (13) and labeled with carbocyanines (14). Islet B cells (labeled with DiI) and non–B cells (labeled with DiO) were mixed together at a ratio of 40% B cells and 60% non–B cells, and placed in culture in the presence or absence of mouse recombinant TNF-α. After 5 d, numerous pseudoislets were observed in each sample. Pseudoislet formation was followed by conventional light microscopy (Fig. 1, *A, C,* and *E*), whereas confocal fluorescent microscopy was used to assess segregation between cell types (Fig. 1, *B, D,* and *F*). Control pseudoislets display a characteristic compact configuration with smooth borders (*A*). Under the confocal microscope the segregation between B cells (red) and non–B cells (green) is striking, with the non–B cells restricted to the periphery of the microorgan (*B*). By contrast, islet cells exposed to TNF-α during the 5 d of reaggregation, produced clusters with rugged borders (*C*), and grossly perturbed cell type segregation (*D*). Aggregates previously exposed to TNF-α for 5 d were then transferred to fresh medium without the cytokine, and cultured for an additional 3 d. As shown in the right panels, they fully recovered the typical shape of control pseudoislets (*E*), with the characteristic cell type segregation (*F*), demonstrating that the effect of TNF-α on islet architecture was fully reversible.

Glucose-stimulated insulin secretion from pseudoislets. To evaluate the functional consequences of long-term (5-d) exposure of islet cells to TNF-α, control and TNF-α–exposed pseudoislets were incubated with 2.8 and 16.7 mM glucose during two successive 90-min incubation periods to measure basal and stimulated insulin secretion, respectively. There was no TNF-α present for either groups during these two assay periods. Basal (2.8 mM glucose) insulin release was slightly elevated from pseudoislets formed in the presence of TNF-α as compared to control (Fig. 2 *A:* 2.4±0.1% vs 1.6±0.1%; $P < 0.005$). When the glucose concentration in the stimulation medium was raised to 16.7 mM, insulin secretion was stimulated 5.5-fold in the control samples (Fig. 2 *A:* 8.9±1.7% vs 1.6±0.1%) but only 2.4-fold in TNF-α–exposed pseudoislets (Fig. 2 *A:* 5.8±1% vs 2.4±0.1%). Interestingly, TNF-α–exposed pseudoislets that recovered normal cellular architecture over an additional 3-d period without the cytokine showed a normalization of both basal and stimulated insulin secretion (Fig. 2 *B*).

Short-term aggregation assay. There is growing evidence that quantitative and qualitative differences in expression of cell adhesion molecules are responsible for segregation between cell types (26, 31). CAMs are cell surface glycoproteins commonly divided into two main classes according to their functional dependence upon cations (32–35). To gain more insight into the molecular basis of the perturbing effect of TNF-α on islet cell type organization, short term aggregation assays of purified islet B cells and non–B cells were performed in the presence or absence of Ca^{2+}. For control B cells, almost no aggregation was observed in the absence of Ca^{2+} (Fig. 3 *B*), while extensive aggregation occurred in its presence (Fig. 3 *A*). By contrast, in B cells treated with TNF-α some aggregation did occur in the absence of Ca^{2+} (Fig. 3 *D*), although still inferior to that seen in the presence of Ca^{2+} (Fig. 3 *C*). This finding suggests the induction by TNF-α of functional Ca^{2+}-independent CAMs at the surface of B cells. No qualitative effect of TNF-α was seen on aggregation of either non–B cells or a 40:60% mixture of B/non–B cells (same ratio as used for pseudoislets) (data not shown).

This qualitative appreciation of the phenomenon was confirmed quantitatively by comparing the number of events at the end of the aggregation period with the starting conditions, which is a classical means of quantifying aggregation (36). As expected from our previous studies (13, 14), in the presence of Ca^{2+} (Fig. 4 *A, white bars*) there was no difference between the aggregation of B and non–B cells (68.7±1.2% compared to 70±3%, NS). Preexposure to TNF-α (Fig. 4 *A, hatched bars*) had no significant influence on these levels (72.5±0.8% and 72.1±1%), probably because aggregation was already maximal in both cell types. When the two cell populations were aggregated in the absence of Ca^{2+} (0.5 mM EGTA) (Fig. 4 *B, white bars*), B cell aggregation only amounted to 24±1.1%, while non–B cell aggregation reached 62.1±1.3%. Pretreatment with TNF-α (Fig. 4 *B, hatched bars*) resulted in a significant increase in Ca^{2+}-independent aggregation of B cells, from 24±1.1% to 44.3±1.2% ($n = 4$, $P < 0.001$), suggesting an induction of Ca^{2+}-independent cell adhesion molecules by the cytokine. By contrast, preexposure to TNF-α had no signifi-

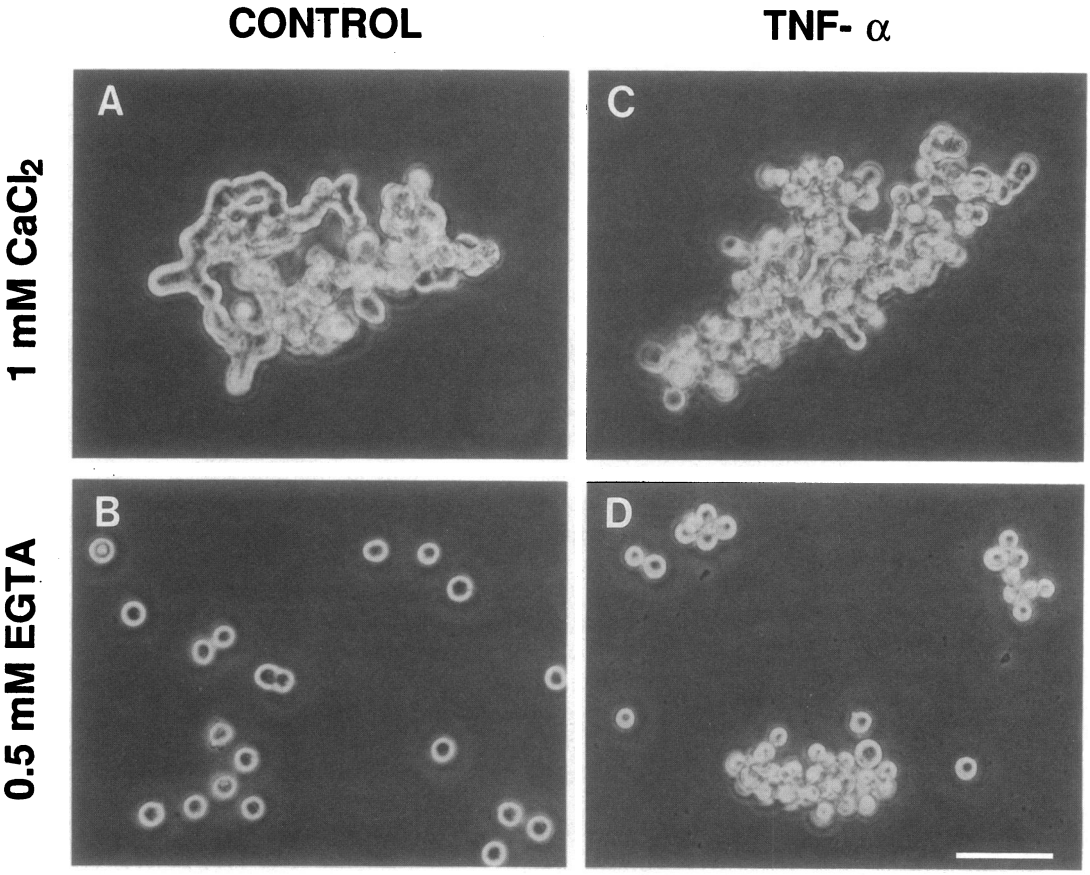

Figure 3. Short-term aggregation assay. Qualitative changes in aggregation properties of B cells treated with TNF-α. Sorted B cells were cultured for 20 h in the absence or in the presence of 100 U/ml TNF-α, at a dilution preventing spontaneous aggregation. They were then concentrated and incubated for 45 min under standardized conditions (see Methods). Aggregation was evaluated by conventional phase contrast microscopy. In the presence of 1 mM $CaCl_2$ (*A* and *C*), no major qualitative difference in aggregation could be observed in cells treated with TNF-α (*C*), compared to control (*A*). In the absence of Ca^{2+} (0.5 mM EGTA) (*B* and *D*), no aggregation occurred in control cells (*B*), while some aggregation was observed in cells treated with TNF-α (*D*), suggesting the induction of functional Ca^{2+}-independent CAMs at the surface of these cells. The figure is representative of four independent experiments. Bar, 60 μm.

cant effect on short-term aggregation of non–B cells in the absence of Ca^{2+} (62.8±4.4% compared to 62.1±1.3%), most likely because of the constitutively high Ca^{2+}-independent adhesion of this cell type.

Experiments were also performed using a 40:60% mixture of B and non–B cells (the same ratio as used for the pseudoislets experiments). As expected from the qualitative data, no effect of TNF-α was measured in short-term aggregation of the mixture of B and non–B cells, either in the presence or absence of calcium (data not shown).

TC treatment (selective removal of Ca^{2+}-independent CAMs). To verify that the increased adhesion of B cells exposed to TNF-α was really caused by an induction of Ca^{2+}-independent CAMs, we tested the adhesion properties of control and TNF-α–exposed B cells after selectively removing Ca^{2+}-independent CAMs from their surface, according to Takeichi et al. (30) (TC treatment, see Methods). As expected, this treatment had no significant effect on Ca^{2+}-dependent aggregation (Fig. 5 *A*), thus demonstrating its specificity. In the absence of Ca^{2+} (Fig. 5 *B*), the aggregation of both control (24±1.1%) and TNF-α–exposed B cells (44.3±1.2%) was completely abolished by TC treatment (8.6±0.4%, and 8.5±0.2%, respectively) supporting the hypothesis that the cytokine might act by inducing the expression of Ca^{2+}-independent adhesion molecules on the surface of B cells. We assume that the recorded 8% "aggregation" obtained in the absence of Ca^{2+} after selective removal of Ca^{2+}-independent CAMs is caused by nonspecific adhesive events and/or by the loss of some cells during the aggregation assay. It is reassuring to see that this value is not different in cells exposed to TNF-α.

TE treatment (selective removal of Ca^{2+}-dependent CAMs). As reported (14), the incubation of islet cells with a low dose of trypsin (1 μg/ml) in the absence of calcium allows for selective removal of the Ca^{2+}-dependent CAMs from the cell surface. We used this approach to demonstrate that the effect of TNF-α on Ca^{2+}-independent adhesion of islet B cells is not an artefact caused by the absence of calcium in the aggregation assay. Such a treatment, by removing Ca^{2+}-dependent CAMs, allowed us to test adhesion strictly mediated by Ca^{2+}-independent CAMs even in the presence of calcium. As already discussed, no effect of TNF-α could be detected on control B cells in the presence of Ca^{2+} (Fig. 6, *A*, 68.4±2.4% compared to 65.6±3.2%, NS). In the absence of Ca^{2+} (Fig. 6 *B*), an increase in Ca^{2+}-independent aggregation became apparent in TNF-α–treated B cells (44.6±1.3% in TNF-α–treated samples as compared to 26.2±0.9% in control samples). After inactivation of

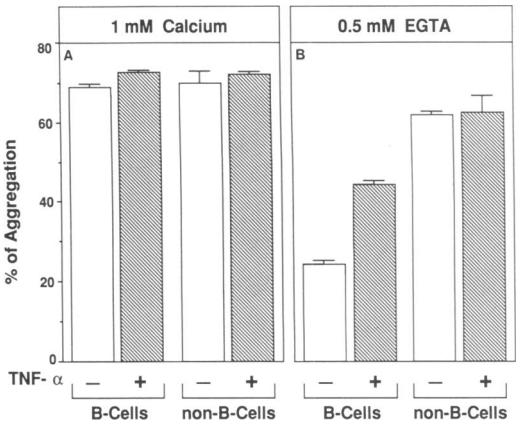

Figure 4. Short-term aggregation assay. Quantitative changes in aggregation properties of B and non–B cells treated with TNF-α. Sorted B and non–B cells were cultured for 20 h in the absence or in the presence of 100 U/ml TNF-α. Short-term aggregation was then quantified (in the absence of TNF-α) by comparing the number of events in aliquots of cell suspension taken before and after a 45-min incubation period. In the presence of calcium (*A*), aggregation of TNF-α–treated B and non–B cells (*hatched bars*) was comparable to control cells (*open bars*). In the absence of calcium (*B*), there was a significant increase in adhesion of B cells exposed to TNF-α (*hatched bar*), as compared to control (*open bar*) ($P < 0.001$), whereas no change was observed for non–B cells. Bars represent the mean±SEM of four independent experiments.

Ca^{2+}-dependent CAMs (Fig. 6 *C, TE treatment*), an effect of TNF-α of the same magnitude was observed in the presence of Ca^{2+} (44.3±1.2% in TNF-α–treated samples as compared to 26.8±0.7% in control samples).

The increased Ca^{2+}-independent adhesion of B cells induced by TNF-α is not mediated by NCAM or ICAM-1. We previously reported that NCAM is highly expressed on islet non–B cells compared to B cells (13). We, therefore, tested whether the increased Ca^{2+}-independent aggregation of TNF-α–exposed B cells was possibly caused by an upregulation of NCAM expression. Using anti-NCAM antibodies, flow cytometric analysis of cells treated with TNF-α did not show any modification of NCAM immunoreactivity compared to control B cells (data not shown). Immuno–flow cytometry analysis further confirmed the induction by TNF-α of ICAM-1 (20, 21), but not LFA-1 molecules, on rat islet B cells (data not shown). Thus, in the absence of the natural ligand of ICAM-1 (i.e., LFA-1), it was not surprising to find that blocking monoclonal antibodies against either ICAM-1 or LFA-1 did not prevent the effect of TNF-α on Ca^{2+}-independent aggregation of B cells (see Table I). Furthermore, anti-NCAM Fab fragments did not mask the effect of TNF-α on B cell short term aggregation in the absence of calcium (Table I). These negative findings suggest the induction by TNF-α of as yet unidentified and possibly novel Ca^{2+}-independent CAMs on islet B cells.

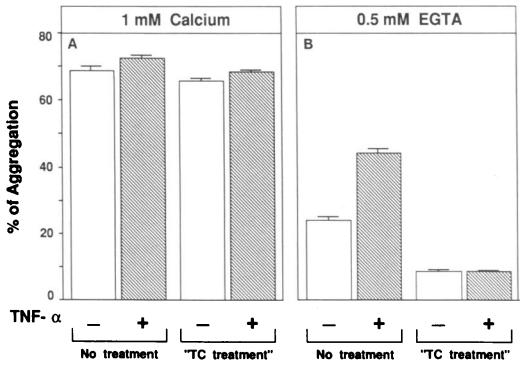

Figure 5. Short-term aggregation assay. The effect of TNF-α is abolished by TC treatment of islet B cells. Treatment of islet cells with trypsin in the presence of calcium (*TC treatment*) had no effect on Ca^{2+}-dependent aggregation (*A*) of both control (*white bars*) and TNF-α–treated cells (*hatched bars*), while specifically removing Ca^{2+}-independent cell adhesion (*B*). The finding that the TNF-α–induced Ca^{2+}-independent aggregation is abolished by TC treatment (*B*), further strengthens the hypothesis that the cytokine may act by inducing and/or activating Ca^{2+}-independent adhesion molecules. Bars represent the mean±SEM of four independent experiments.

Discussion

Previous studies have shown that the topological cell relationships described in normal islets is disturbed in all forms of diabetes. In insulin-dependent diabetes mellitus (IDDM), the islet looks like a random mixture of non–B cells (3); in diabetic mice, Orci et al. have observed penetration of the residual B cell core by D cells (4). In Stilman Salgado (eSS) rats, a disruption of islet architecture precedes B cell destruction, but coincides with the onset of glucose intolerance (6). In animal models of non–insulin-dependent diabetes mellitus (NIDDM) (db/db or ob/ob mice), the hyperplasia of B cells is such that the rim of non–B cells is completely dismantled (5). It has further been found that in ob+/ob+ mice a profound pertur-

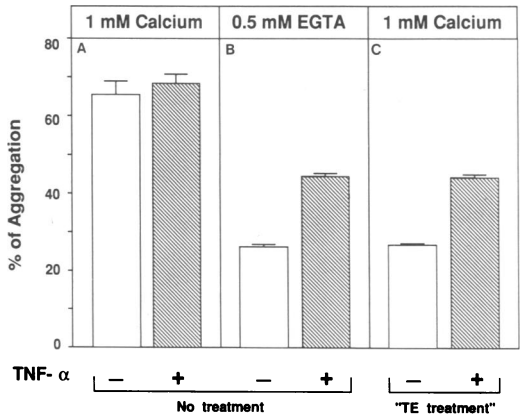

Figure 6. Short term aggregation assay. Inactivation of Ca^{2+}-dependent CAMs (*0.5 mM EGTA* or *TE treatment*) is necessary to disclose the effect of TNF-α on short term aggregation of B cells. Preexposure of B cells to TNF-α is apparently without effect on short-term aggregation of B cells in the presence of Ca^{2+} (*A*). After inactivation of Ca^{2+}-dependent CAMs, however, either by removal of Ca^{2+} (*B*) or TE treatment (*C*), a significant ($P < 0.001$) effect on adhesion is disclosed, suggesting that TNF-α acts by increasing the expression/activity of Ca^{2+}-independent CAMs, either in the presence or absence of Ca^{2+}. Bars represent the mean±SEM of four independent experiments.

Table I. Effect of Specific Antibodies (or Fab Fragments) on Ca^{2+}-independent Aggregation of Control and TNF-α-treated B Cells

Antibodies	ICAM-1 $n = 4$	LFA-1α $n = 4$	LFA-1β $n = 4$	Fab fragments	NI $n = 2$	NCAM $n = 2$
Control	27.8±1.2	27.1±2.5	26.7±1.1	Control	25.3±0.7	26.3±0.7
TNF-α	44.7±0.9*	44.3±1.2‡	44.2±1.1‡	TNF-α	43.1±0.1	42.8±0.9

Data represent the percentages of Ca^{2+}-independent aggregation obtained in the short term aggregation assay in the presence of the indicated antibodies or Fab fragments (see Methods for details). For ICAM-1, LFA-1α, and LFA-1β experiments, values are expressed as mean±SEM of four separate experiments (* $P < 0.0001$; ‡ $P < 0.005$). Values for NCAM experiments are expressed as mean±SD ($n = 2$). NI, nonimmune.

bation of islet architecture accompanies the onset of the diabetic syndrome within 20 wk of birth (7). It has been proposed that such islet structural disturbance might significantly contribute to the dysregulation of glucagon (in IDDM) or insulin (in NIDDM) secretion (2). Since recent studies have emphasized a possible role of TNF-α in the early physiopathological events leading to IDDM (17, 19), we wanted to assess whether TNF-α might jeopardize the integrity of islet structure.

The ability of isolated islet cells to reaggregate in organoids displaying a three-dimensional cell type organization similar to that of native islets (8–10, 14) provided a good model system to study the possible effects of TNF-α on islet cell type segregation. The study shows that a mixture of isolated islet cells is still able to form clusters in the presence of TNF-α, but that the typical segregation between B and non–B cells does not occur. This effect occurred at a dose of TNF-α known to be nontoxic to islet cells (37–39), and was reversed after removal of the cytokine from the incubation medium, suggesting a true regulatory effect on cell adhesion.

Insulin secretion of aggregates formed in the presence of TNF-α was characterized by an increased basal secretion and a decreased response to glucose, compared to control pseudoislets. The effect was also fully reversible. The same pattern of changes has been observed in the past with dissociated B cells, compared to intact islets or to pseudoislets (40–45). Our finding is thus consistent with the hypothesis that a disordered islet architecture might result in the loss of intraislet regulation of insulin secretion. Nevertheless, we cannot exclude the possibility of a direct effect on insulin secretion of TNF-α, even at such a low dose (38, 39). Other ways of perturbing islet cell type organization will therefore be needed to confirm a direct role of islet organization in islet function.

Cell adhesion molecules have been established to play an important role in the formation and maintenance of tissue structure (34). As shown by CAM transfection studies, both quantitative or qualitative differences in CAM expression result in segregation between clones in culture (26, 31). Also, perturbation of CAM expression results in remodeling of the three-dimensional organization of tissues (35). The same principles might govern the reconstitution of islet-like organoids (pseudoislets) from a mixture of dissociated islet cells in vitro. It has been recognized that CAMs fall into two general classes of molecules: the Ca^{2+}-dependent and the Ca^{2+}-independent CAMs, which can both coexist on the same cell (32–35). We previously reported that strictly calcium-dependent aggregation mechanisms were equally efficient on both B cells and non–B cells, while Ca^{2+}-independent mechanisms were much more prominent on non–B cells (13). Perturbation experiments with anti-CAM Fab fragments suggested to us that the difference in expression of Ca^{2+}-independent CAMs was responsible for islet cell type segregation (14).

The present results show that preincubation with TNF-α increased the aggregation of B cells in the absence of Ca^{2+}, suggesting that the cytokine induced the expression of Ca^{2+}-independent CAMs on these cells. This hypothesis is supported by the demonstration that the effect was abolished by the removal of this class of molecules from the surface of B cells (TC treatment). This test is the only available means of selectively removing Ca^{2+}-independent CAMs. The fact that aggregation in the presence of calcium was not modified, and that aggregation of both B and non–B cells in the absence of calcium was similarly abolished by TC treatment attest for the specificity and the sensitivity of this widely used test (14, 30, 33, 46–48).

Although the study of aggregation in the absence of calcium is a classical means of assessing possible involvement of Ca^{2+}-independent CAMs, it is nonphysiological. To circumvent this flaw, strictly Ca^{2+}-dependent CAMs were inactivated by TE treatment, allowing the inductive effect of TNF-α on Ca^{2+}-independent CAMs to be disclosed even in the presence of Ca^{2+}.

It has been shown that TNF-α can induce the expression of ICAM-1 on human islet B cells (20, 21). This was confirmed on rat cells in the course of the present study. Although ICAM-1 is a Ca^{2+}-independent CAM, and shares some homology with NCAM (both belonging to the immunoglobulin superfamily) (49, 50), we doubted that it could be responsible for the effect of TNF-α on B cell aggregation for the following reasons: (*a*) the integrin LFA-1, which is the ICAM-1 ligand (51, 52), is not expressed on B cells as assessed by flow cytometry, using anti LFA-1 (against α and β subunits) antibodies; (*b*) another member of the LFA-1 family of integrins is probably not involved, since an antibody against the common β subunit neither revealed the molecule by flow cytometry, nor prevented the effect of TNF-α on short term aggregation; and (*c*) finally, an anti–rat ICAM-1 antibody did not prevent the effect of TNF-α on short-term B cell aggregation. This last finding also excludes the possibility that ICAM-1 may provide homophilic adhesion between cells, as is the case for other CAMs belonging to the immunoglobulin superfamily (49, 50). Among these, NCAM was shown to be expressed on islet cells, with higher concentration on non–B cells (13). Its expression on B cells was not, however, modified by TNF-α.

Whether there is a direct cause–effect relationship between the increase in Ca^{2+}-independent aggregation of B cells and the

altered cell type segregation induced by TNF-α cannot be affirmed yet. One might have expected that randomization of B cells within pseudoislets be associated with a decreased affinity between B cells. However, according to our previous studies demonstrating the crucial role of Ca^{2+}-independent CAMs in islet cell type segregation (14), and the transfection studies mentioned above, it is reasonable to think that an increased level of Ca^{2+}-independent CAMs on B cells would attenuate the differences in aggregation properties between cell types, thereby affecting segregation within pseudoislets in vitro.

Cell adhesion and segregation are also dependent on functional microtubules and microfilaments of the cytoskeleton (53). It is unlikely that part of the effect of TNF-α is secondary to an altered cytoskeleton function, since cell cluster formation and short-term aggregation are not impaired.

In conclusion, the present study shows that TNF-α increases Ca^{2+}-independent aggregation of islet B cells and prevents the normal segregation between islet cell types during the formation of pseudoislets. This was accompanied by an abnormal insulin secretion. Other ways of perturbing islet architecture will be needed to confirm a direct role of islet organization in islet function. Nonetheless, the observed effects of a cytokine on islet structure and function might represent an additional pathway in the cascade of events leading to islet functional defects in diabetes.

Acknowledgments

We are indebted to Françoise Mottaz, Florence Théraulaz, and Karine Baudouin for skillful technical assistance. We also thank Dr. U. Rutishauser, Dr. T. Tamatani, and Dr. M. Miyasaka, who generously supplied the specific antisera, BASF & Knoll (Ludwigshafen, Germany) for providing mouse recombinant TNF-α, Dr. D. Janjic for helpful discussions, and D. Wohlwend for flow cytometry technical advice.

V. Cirulli is the recipient of a Juvenile Diabetes Foundation International postdoctoral fellowship. This work was supported by Swiss National Science Fund grants 31-9394.88, 32-31307.91, and 32-8917.86.

References

1. Orci, L., and R. Unger. 1975. Functional subdivision of islets of langerhans and possible role of D-cells. *Lancet.* ii:1243–1244.

2. Orci, L. 1978. Insulin, glucagon and somatostatin secretion in the regulation of metabolism. *Ann. Rev. Physiol.* 40:307–343.

3. Unger, R. H., and L. Orci. 1981. Glucagon and the A-cell. Physiology and pathophysiology. *New Engl. J. Med.* 304:1575–1580.

4. Orci, L., D. Baetens, C. Rufener, M. Amherdt, M. Ravazzola, P. Studer, F. Malaisse-Lagae, and R. Unger. 1976. Hypertrophy and hyperplasia of somatostatin-containing D-cells in diabetes. *Proc. Natl. Acad. Sci. USA.* 73:1338–1342.

5. Baetens, D., Y. Stefan, M. Ravazzola, F. Malaisse-Lagae, D. L. Coleman, and L. Orci. 1978. Alteration of islet cell populations in spontaneously diabetic mice. *Diabetes.* 27:1–7.

6. Gomez Dumm, C. L. A., M. C. Semino, and J. J. Gagliardino. 1990. Sequencial morphological changes in pancreatic islets of spontaneously diabetic rats. *Pancreas.* 5:533–539.

7. Starich, G. H., M. Zafirova, R. Jablenska, P. Petkov, and C. K. Lardinois. 1991. A morphological and immunohistochemical investigation of endocrine pancreata from obese ob+/ob+ mice. *Acta Histochem.* 90:93–101.

8. Montesano, R., P. Mouron, M. Amherdt, and L. Orci. 1983. Collagen matrix promotes reorganization of pancreatic endocrine cell monolayers into islet-like organoids. *J. Cell Biol.* 97:935–939.

9. Hopcroft, D. W., D. R. Mason, and R. S. Scott. 1985. Insulin secretion from perifused pancreatic pseudoislets. *In Vitro Cell. & Dev. Biol.* 21:421–427.

10. Halban, P. A., S. L. Powers, K. L. George, and S. Bonner-Weir. 1987. Spontaneous reassociation of dispersed adult rat pancreatic islet cells into aggregates with three-dimensional architecture typical of native islets. *Diabetes.* 36:783–790.

11. Tze, W. J., and J. Tai. 1982. Preparation of pseudoislets for morphological and functional studies. *Transplantation (Baltimore).* 34:228–231.

12. Ono, J., R. Takaki, H. Okano, and M. Fukuma. 1979. Long-term culture of pancreatic islet cells with special reference to β-cell function. *In Vitro (Rockville).* 15:95–102.

13. Rouiller, G. D., V. Cirulli, and P. A. Halban. 1990. Differences in aggregation properties and levels of the neural cell adhesion molecule (NCAM) between islet cell types. *Exp. Cell Res.* 191:305–312.

14. Rouiller, G. D., V. Cirulli, and P. A. Halban. 1991. Uvomorulin mediates calcium-dependent aggregation of islet cells, whereas calcium-independent cell adhesion molecules distinguish between islet cell types. *Dev. Biol.* 148:233–242.

15. Dinarello, C. A., and J. W. Mier. 1987. Lymphokines. *N. Engl. J. Med.* 317:940.

16. Le, J., and J. Vilcek. 1987. Tumor necrosis factor and interleukin-1: cytokines with multiple overlapping biological activities. *Lab. Invest.* 56:234.

17. Mandrup-Poulsen, T., K. Bendtzen, C. A. Dinarello, and J. Nerup. 1987. Human tumor necrosis factor potentiates human interleukin 1-mediated rat pancreatic β-cell cytotoxicity. *J. Immunol.* 139:4077–4082.

18. Campbell, I. L., A. Iscaro, and L. C. Harrison. 1988. IFN-γ and Tumor necrosis factor-α: cytotoxicity to murine islets of Langerhans. *J. Immunol.* 141:2325–2329.

19. Campbell, I. L., W. H. Kay, L. Oxbrow, and L. C. Harrison. 1991. Essential role for interferon-γ and interleukin-6 in autoimmune insulin-dependent diabetes in NOD/Wehi mice. *J. Clin. Invest.* 87:739–742.

20. Campbell, I. L., A. Cutri, D. Wilkinson, A. W. Boyd, and L. C. Harrison. 1989. Intercellular adhesion molecule 1 is induced on isolated endocrine islet cells by cytokines but not by reovirus infection. *Proc. Natl. Acad. Sci. USA.* 86:4282–4286.

21. Vives, M., G. Soldevila, L. Alcade, C. Lorenzo, N. Somoza, and R. Pujol-Borrel. 1991. Adhesion molecules in human islet β-cells. De novo induction of ICAM-1 but not LFA-3. *Diabetes.* 40:1382–1390.

22. Sutton, R., M. Peters, P. Mcshane, D. W. Gray, and P. J. Morris. 1986. Isolation of rat pancreatic islets by ductal injection of collagenase. *Transplantation (Baltimore).* 42:689–691.

23. Loken, M., and L. Herzenberg. 1975. Analysis of cell populations with a fluorescence-activated cell sorter. *Ann. NY Acad. Sci.* 254:163–171.

24. Van De Winkel, M., E. Maes, and D. Pipeleers. 1982. Islet cell analysis and purification by light scatter and autofluorescence. *Biochem. Biophys. Res. Commun.* 107:525–532.

25. Coons, A., E. Leduc, and J. Connolly. 1955. Studies on antibody production. I. A method histochemical demonstration of specific antibody and its application to a study of the hyperimmune rabbit. *J. Exp. Med.* 102:49–63.

26. Friedlander, D. R., R. M. Mege, B. A. Cunningham, and G. M. Edelman. 1989. Cell sorting-out is modulated by both the specificity and amount of different cell adhesion molecules (CAMs) expressed on cell surfaces. *Proc. Natl. Acad. Sci. USA.* 86:7043–7047.

27. Honig, M. G., and R. I. Hume. 1989. DiI and DiO: versatile fluorescent dyes for neuronal labelling and pathway tracing. *TINS (Trends Neurosci.)* 12:333–341.

28. Petersen, C. M., A. Nykjaer, B. S. Christiansen, L. Heickendorff, S. C. Mogensen, and B. Moller. 1989. Bioactive human recombinant tumor necrosis factor-α: an unstable dimer? *Eur. J. Immunol.* 19:1887–1894.

29. Tamatani, T., M., Kotani, and M. Miyasaka. 1991. Characterization of the rat leukocyte integrin, CD11/CD18, by the use of LFA-1 subunit-specific monoclonal antibodies. *Eur. J. Immunol.* 21:627–633.

30. Takeichi, M., H. S. Ozaki, K. Tokunaga, and T. S. Okada. 1979. Experimental manipulation of cell surface to affect cellular recognition mechanisms. *Dev. Biol.* 70:195–205.

31. Nose, A., A. Nagafuchi, and M. Takeichi. 1988. Expressed recombinant cadherins mediate cell sorting in model systems. *Cell.* 54:993–1001.

32. Urushihara, H., M. J. Ueda, T. S. Okada, and M. Takeichi. 1977. Calcium-dependent and calcium-independent adhesion of normal and transformed BHK cells. *Cell Struct. Funct.* 2:289–296.

33. Takeichi, M. 1977. Functional correlation between cell adhesive properties and some cell surface proteins. *J. Cell Biol.* 75:464–474.

34. Edelman, G. M. 1986. Cell adhesion molecules in the regulation of animal form and tissue pattern. *Ann. Rev. Cell Biol.* 2:81–116.

35. Edelman, G. M., and K. Crossin. 1991. Cell adhesion molecules: implication for a molecular histology. *Annu. Rev. Biochem.* 60:155–190.

36. Brackenbury, R., J. P. Thiery, U. Rutishauser, and G. M. Edelman. 1977. Adhesion among neural cells of the chick embryo. *J. Biol. Chem.* 252:6835–6840.

37. Rabinovich, A., H. Baquerizo, C. Pukel, and W. Sumoski. 1989. Effects of cytokines on rat pancreatic islet cell monolayer cultures: distinction between functional and cytotoxic effects on islet β-cells. *Reg. Immunol.* 2:77–82.

38. Rabinovitch, A., W. L. Suarez, P. D. Thomas, K. Strynadka, and I. Simpson. 1992. Cytotoxic effect of cytokines on rat islets: evidences for involvement of free radicals and lipid peroxidation. *Diabetologia.* 35:409–413.

39. Pukel, C., H. Baquerizo, and A. Rabinovitch. 1988. Destruction of rat islet cell monolayers by cytokines. *Diabetes.* 37:133–136.

40. Lernmark, A. 1974. The preparation of, and studies on, free cell suspensions from mouse pancreatic islets. *Diabetologia.* 10:431–438.

41. Halban, P. A., C. Wollheilm, B. Blondel, P. Meda, E. N. Nierson, and D. H. Mintz. 1982. The possible importance of contact between pancreatic islet cells for the control of insulin release. *Endocrinology.* 111:86–94.

42. Pipeleers, D., P. In't Veld, E. Maes, and M. Van De Winkel. 1982. Glucose-induced insulin release depends on functional cooperation between islet cells. *Proc. Natl. Acad. Sci. USA.* 79:7322–7325.

43. Schröder, D., U. Wegner, W. Besch, and H. Zühlke. 1983. Characterization of pseudo-islets formed from pancreatic islet cell suspensions of neonatal rats. *Mol. Cell. Endocrinol.* 32:179–193.

44. Weir, G. C., P. A. Halban, P. Meda, C. Wollheilm, L. Orci, and A. E. Renold. 1984. Dispersed adult rat pancreatic islet cells in culture: A, B, and D cell function. *Metabolism.* 33:447–453.

45. Pipeleers, D., F. C. Schuit, P. A. In't Veld, E. Maes, E. L. Hooghe-Peters, M. Van De Winkel, and W. Gepts. 1985. Interply of nutrients and hormones in the regulation of insulin release. *Endocrinology.* 117:824–833.

46. Ozawa, M., and R. Kemler. 1990. Correct proteolytic cleavage is required for the cell adhesive function of uvomorulin. *J. Cell Biol.* 111:1645–1650.

47. Hyafil, F., C. Babinet, and F. Jacob. 1981. Cell-cell interactions in early embryogenesis: a molecular approach to the role of calcium. *Cell.* 26:447–454.

48. Gallin, W. J., G. M. Edelman, and B. A. Cunningham. 1983. Characterization of L-CAM, a major cell adhesion molecule from embryonic liver cells. *Proc. Natl. Acad. Sci. USA.* 80:1038–1042.

49. Staunton, D. E., S. D. Marlin, C. Stratowa, M. L. Dustin, and T. A. Springer. 1988. Primary structure of ICAM-1 demonstrates interaction between members of the immunoglobulin and integrin supergene families. *Cell.* 52:925–933.

50. Simmons, D., M. W. Makgoba, and B. Seed. 1988. ICAM, an adhesion ligand of LFA-1, is homologous to the neural cell adhesion molecule NCAM. *Nature (Lond.).* 331:624–627.

51. Marlin, S. D., and T. A. Springer. 1987. Purified intercellular adhesion molecule-1 (ICAM-1) is a ligand for lymphocyte function-associated antigen-1 (LFA-1). *Cell.* 51:813–819.

52. Makgoba, M. W., M. E. Sanders, G. E. Ginther Luce, M. L. Dustin, T. A. Springer, E. A. Clark, P. Mannoni, and S. Shaw. 1988. ICAM-1 a ligand for LFA-1-dependent adhesion of B, T and myeloid cells. *Nature (Lond.).* 331:86–88.

53. Jaffe, S. H., D. R. Friedlander, F. Matsuzaki, K. L. Crossin, B. A. Cunningham, and G. M. Edelman. 1990. Differential effects of the cytoplasmic domains of cell adhesion molecules on cell aggregation and sorting-out. *Proc. Natl. Acad. Sci. USA.* 87:3589–3593.